

**EVALUATION OF STRENGTH
CHARACTERISTICS OF MORTAR AND
CONCRETE DURING CURING USING EMI
AND SURFACE WAVE PROPAGATION
TECHNIQUES**



NELLY BINTI MAJAIN

UMS
UNIVERSITI MALAYSIA SABAH

**FACULTY OF ENGINEERING
UNIVERSITI MALAYSIA SABAH
2016**

**EVALUATION OF STRENGTH
CHARACTERISTICS OF MORTAR AND
CONCRETE DURING CURING USING EMI
AND SURFACE WAVE PROPAGATION
TECHNIQUES**



NELLY BINTI MAJAIN

UMMS

**THESIS SUBMITTED IN FULFILLMENT FOR
THE DEGREE OF MASTER OF ENGINEERING**

**FACULTY OF ENGINEERING
UNIVERSITI MALAYSIA SABAH
2016**

DECLARATION

I hereby declare that the material in this thesis is my own except for quotations, excerpts, equations, summaries and references, which have been duly acknowledged.

26 January 2016

Nelly Binti Majain
MK 1211008T



UMS
UNIVERSITI MALAYSIA SABAH

CERTIFICATION

NAME : **NELLY BINTI MAJAIN**

MATRIC NO. : **MK 1211008T**

TITLE : **EVALUATION OF STRENGTH CHARACTERISTICS OF MORTAR AND CONCRETE DURING CURING USING EMI AND SURFACE WAVE PROPAGATION TECHNIQUES**

DEGREE : **MASTER OF ENGINEERING (CIVIL ENGINEERING)**

VIVA DATE : **05 OCTOBER 2015**



DECLARED BY

UMS
UNIVERSITI MALAYSIA SABAH

1. MAIN SUPERVISOR

Assoc. Prof. Dr. Willey Liew Yun Hsien

Signature

2. CO-SUPERVISOR

Dr. Lim Yee Yan

ACKNOWLEDGEMENTS

First and foremost I would like to thank God for giving me the strength and grace to complete this thesis. I am nothing without Him.

I would like to express my sincere gratitude to my supervisor Assoc. Prof. Dr. Willey Liew Yun Hsien for being so understanding, kind, patient, generous and caring throughout my study period. Thank you for believing in me and for your willingness to take me as your student.

A special thank you to my co-supervisor Dr. Lim Yee Yan who contributed to the original idea of this thesis. Thank you for being so generous and for guiding me throughout these years. I am grateful that you have helped me so much in sharing your knowledge and information. Thank you also for sharing and allowing me to use some of your great research works.

I am also grateful to Prof. Ir. Dr. Abdul Karim Mirasa who always encouraged me to complete my studies. To all the technicians in the Concrete Laboratory, Electric and Electronic Lab and staff at the Faculty of Engineering, thank you for all your help and kind assistance. I would also like to thank my friends, Joel, Charles and the final year students for helping me out in conducting the experiments.

This thesis would not have been completed without the support of my family. I would like to thank my beloved parents and siblings (Genevive, Jonas, Regina, Sr. Marie Carmen and Emily) for their understanding and for their love and constant prayers.

I am also thankful to my best friend Melissa Nicholas for always encouraging me and believing in me. Thank you for always being there for me throughout all the ups and downs of my life.

Finally, I would like to thank all of my friends in Life Teen as well as my superiors (especially Ir. James Yong Hon Min) and colleagues in PY Konsep Perunding Sdn. Bhd. that have been my communities and sources of joy and support.

Nelly Majain
26 January 2016

ABSTRACT

Concrete is a non-homogenous material with complex microstructure, consisting of water, cement, aggregates and other suitable materials. During concreting of concrete structures, heat will be released due to the hydration process between cement and water. At this stage, curing process is crucial and it needs to be monitored so that the concrete will be able to achieve the desired strength and becomes durable. Due to the complexity of concrete microstructure, the evaluations for concrete curing and strength monitoring are difficult and have moved at a slower pace. However, in recent years the advancements of piezoelectric materials such as Lead Zirconate Titanate (PZT) have attracted interest among researchers to develop new non-destructive evaluation methods to investigate the performance of concrete. The key advantage of using PZT is that it can be placed anywhere even in remote and inaccessible locations as both actuator and sensor to monitor concrete structures. The electromechanical impedance (EMI) and surface wave propagation techniques employing PZT transducer have been developed by researchers as a non-destructive approaches for evaluating concrete. The main objective of this thesis is to evaluate the strength characteristics of mortar and concrete during curing using the EMI and surface wave propagation techniques. In order to achieve this, the research begins with conducting parametric study on free vibration of PZT transducer in the application of EMI technique. The work continues with experimental investigation to study the feasibility of using the EMI and surface wave propagation techniques employing PZT transducer for evaluation of strength characteristics of mortar and concrete during curing. The PZT transducers were attached to the mortar and concrete specimens through surface bonding and embedded methods. The results showed that by using the EMI and surface wave propagation techniques employing the PZT transducer, the duration of concrete setting and curing can be determined. Also, a good correlation between the concrete dynamic modulus of elasticity with compressive strength has been achieved by using the surface wave propagation method. For these reasons, the EMI and surface wave propagation techniques can be a useful tools to ensure the safety and quality of concrete structures during construction and service.

ABSTRAK

PENILAIAN CIRI-CIRI KEKUATAN MORTAR DAN KONKRIT SEMASA PENGAWETAN MENGGUNAKAN TEKNIK EMI DAN PERAMBATAN GELOMBANG PERMUKAAN

Konkrit merupakan bahan yang tidak homogen dengan mikrostruktur yang kompleks dan yang terdiri daripada air, simen, agregat dan bahan-bahan lain yang sesuai. Semasa kerja menuang konkrit dalam pembinaan struktur konkrit, haba akan dibebaskan melalui proses penghidratan di antara simen dan air. Pada peringkat ini, proses pengawetan adalah penting dan ia perlu dipantau supaya konkrit akan dapat mencapai kekuatan yang dikehendaki dan menjadi tahan lama. Oleh kerana konkrit mempunyai mikrostruktur yang kompleks, penilaian untuk pengawetan konkrit dan pemantauan kekuatan adalah sukar dan bergerak dengan kadar perlahan. Walau bagaimanapun, beberapa tahun kebelakangan ini, kemajuan bahan-bahan piezoelektrik seperti 'Lead Zirconate Titanate' (PZT) telah menarik minat kalangan penyelidik untuk membina teknik-teknik penilaian ujian tanpa musnah yang baru bagi mengkaji prestasi konkrit. Kelebihan utama menggunakan PZT ialah ia boleh diletakkan dimana-mana walaupun di tempat yang jauh dan lokasi yang tidak dapat diakses sebagai aktuator (penggerak) dan sensor (pengesan) untuk mengawasi struktur konkrit. Teknik elektromekanikal impedans (EMI) dan perambatan gelombang permukaan menggunakan transduser PZT telah dibangunkan oleh para penyelidik sebagai pendekatan tanpa musnah untuk penilaian konkrit. Objektif utama tesis ini adalah untuk membuat penilaian terhadap ciri-ciri kekuatan mortar dan konkrit semasa pengawetan menggunakan teknik-teknik EMI dan perambatan gelombang permukaan. Bagi mencapai objektif ini, penyelidikan ini bermula dengan menjalankan kajian parametrik terhadap getaran bebas transduser PZT dalam penggunaan teknik EMI. Penyelidikan diteruskan dengan kajian eksperimen untuk mengkaji kemungkinan menggunakan teknik EMI dan perambatan gelombang permukaan menggunakan PZT transduser untuk penilaian ciri-ciri kekuatan mortar dan konkrit semasa pengawetan. Transduser PZT diletakkan ke atas spesimen mortar dan konkrit melalui ikatan permukaan dan kaedah terbenam. Hasil kajian ini menunjukkan bahawa dengan menggunakan teknik EMI dan perambatan gelombang permukaan menggunakan transduser PZT, tempoh penetapan konkrit dan pengawetan boleh ditentukan. Selain itu, korelasi yang baik antara modulus dinamik keanjalan konkrit dengan kekuatan mampatan telah dicapai menggunakan kaedah perambatan gelombang permukaan. Oleh sebab itu, teknik EMI dan perambatan gelombang permukaan boleh menjadi kaedah yang berguna untuk memastikan keselamatan dan kualiti struktur konkrit semasa pembinaan dan perkhidmatan.

TABLE OF CONTENTS

	Pages
TITLE	i
DECLARATION	ii
CERTIFICATION	iii
ACKNOWLEDGEMENTS	iv
ABSTRACT	v
<i>ABSTRAK</i>	vi
LIST OF CONTENTS	vii
LIST OF TABLES	xii
LIST OF FIGURES	xiii
LIST OF ABBREVIATIONS	xix
LIST OF SYMBOLS	xx
LIST OF APPENDICES	xxiii
CHAPTER 1: INTRODUCTION	1
1.1 Introduction	1
1.2 Objectives and Scopes	5
1.3 Research Contributions	6
1.4 Thesis Organization	7
CHAPTER 2: LITERATURE REVIEW	9
2.1 Overview of Structural Health Monitoring	9
2.2 Common test for Concrete Materials	10
2.2.1 Cement Testing	10
2.2.2 Fine and Coarse Aggregate Testing	12
2.2.3 Water Testing	12
2.3 Concrete Hydration Process and Curing of Concrete	12
2.3.1 Conventional Test for Concrete Hydration	14

2.4	Conventional Evaluation Methods for Concrete Curing and Strength Monitoring	15
2.4.1	Compressive Strength of Concrete Cubes Method	15
2.4.2	Concrete Flexural Strength Method	17
2.4.3	Rebound Hammer Method	17
2.4.4	Windsor Probe Method	18
2.4.5	Maturity Method	19
2.4.6	Ultrasonic Pulse Velocity	19
2.4.7	Stress-Wave Propagation Methods	20
2.4.8	Summary of Conventional Evaluation Methods for Concrete Curing and Strength Monitoring	21
2.5	Application of smart materials in SHM	21
2.6	Piezoelectricity and Piezoelectric Materials	22
2.6.1	Background	22
2.6.2	Fundamentals of Piezoelectric Materials	23
2.6.3	Piezoelectric Constitutive Relations	24
2.6.4	Classifications of Piezoelectric Materials	28
	a. Piezoceramics	28
	b. Piezopolymers	30
2.6.5	Smart Materials: Current and Future Prospects	31
2.7	Application of Electromechanical Impedance (EMI) Technique in SHM	32
2.7.1	Physical Principles of EMI Technique	32
2.7.2	Concrete Hydration Monitoring using EMI technique	35
2.7.3	Advantages of EMI Technique	37
2.7.4	Limitations of EMI Technique in Concrete Hydration Monitoring	37
2.8	Analytical Modeling of EMI Technique	38
2.9	Concrete Strength and Hydration Monitoring using Wave Propagation Technique	42
2.9.1	Stress Wave Propagation Principles	44
2.9.2	Piezoelectric Transducers for Ultrasonic Wave Generation	47

2.9.3	Signal Processing Implementation	48
2.10	Future of Integrated Use of EMI and Wave Propagation Techniques for Concrete Hydration and Strength Monitoring	49
2.11	Summary	49
CHAPTER 3: A PARAMETRIC STUDY ON FREE VIBRATION OF PZT TRANSDUCER IN THE APPLICATION OF ELECTROMECHANICAL IMPEDANCE (EMI) TECHNIQUE		51
3.1	Introduction	51
3.2	Materials and Methods	51
3.2.1	Fundamentals of EMI Technique	51
3.2.2	Theoretical Modelling of PZT Transducer	52
3.2.3	Parametric Study of Admittance Signatures	54
3.3	Experimental Setup	56
3.4	Results and Discussion	56
3.5	Summary	69
CHAPTER 4: MONITORING OF MORTAR HYDRATION USING PIEZOELECTRIC BASED ELECTROMECHANICAL IMPEDANCE (EMI) TECHNIQUE		70
4.1	Introduction	70
4.2	Physical Principle of EMI Technique for Mortar Hydration	70
4.3	Experimental Setup	72
4.3.1	Surface Bonded Method	72
4.3.2	Embedded Method	73
4.4	Results and Discussion	75
4.4.1	Surface Bonded Method	75
	a. Early Age Monitoring	76
	b. Hydration Monitoring After 1 Day	78
4.4.2	Embedded Method	81
4.5	Summary	84

CHAPTER 5: MONITORING OF MORTAR DURING CURING USING PIEZOELECTRIC BASED SURFACE WAVE PROPAGATION TECHNIQUE	85
5.1 Introduction	85
5.2 Physical Principle of Surface Wave Propagation Technique	85
5.3 Experimental Setup	88
5.4 Signal Processing	90
5.5 Results and Discussion	95
5.6 Summary	102
CHAPTER 6: EVALUATION OF STRENGTH CHARACTERISTICS OF CONCRETE DURING CURING USING PIEZOELECTRIC BASED SURFACE WAVE PROPAGATION TECHNIQUE	103
6.1 Introduction	103
6.2 Experimental Setup	103
6.3 Results and Discussion	110
6.4 Summary	116
CHAPTER 7: CONCLUSIONS AND RECOMMENDATIONS FOR FUTURE WORKS	117
7.1 Introduction	117
7.2 Review of Objectives	117
7.3 Conclusion of the Parametric Study on Free Vibration of PZT Transducer in the Application of EMI Technique	118
7.4 Conclusion on the Evaluation of Strength Characteristics of Mortar and Concrete during Curing using the EMI and Surface Wave Propagation Techniques	119
7.5 Implication of the Works	120
7.6 Recommendation for Future Works	121
REFERENCES	122
AUTHOR'S PUBLICATIONS	132

APPENDICES

A	MATLAB Code to Calculate the Analytical Value of Electrical Admittance of PZT.	133
B	MATLAB Code to Compute Cross Correlation and Hilbert Transform Methods	135
C	Some experimental results from the Surface Wave Propagation method.	138



UMS
UNIVERSITI MALAYSIA SABAH

LIST OF TABLES

	Pages
Table 2.1: Typical properties of PVDF and PZT	30
Table 3.1: List of PZT's parameters and their corresponding values	55
Table 3.2: Summary of the effects on conductance and susceptance signatures by increasing the values of various PZT's parameters.	67
Table 6.1: Dynamic Modulus of Elasticity and Compression Strength of Concrete Cubes	115



UMS
UNIVERSITI MALAYSIA SABAH

LIST OF FIGURES

	Page
Figure 1.1: Injaka Bridge Collapsed	2
Figure 2.1: Le Chatelier Moulds	11
Figure 2.2: Vicat's Apparatus	11
Figure 2.3: Concrete curing using water and gunny sacks on concrete slab.	13
Figure 2.4: Isothermal Calorimeter Instrument	15
Figure 2.5: Concrete Compressive Test Machine	16
Figure 2.6: Concrete Flexural Test Machine	17
Figure 2.7: Rebound Hammer Device	18
Figure 2.8: Windsor Probe Device	18
Figure 2.9: PUNDIT Instruments for Ultrasonic Pulse Velocity Method.	20
Figure 2.10: Piezoelectric Effect	23
Figure 2.11: A Piezoelectric Element with Conventional Labels of Axes.	26
Figure 2.12: Matrix for PZT and Quartz	26
Figure 2.13: Perovskite structure of PZT	28
Figure 2.14: Various Types of Piezoceramic Materials	29
Figure 2.15: Experimental Setup for EMI Technique	33
Figure 2.16: Typical plot of admittance signature against frequency for an aluminium beam under different health conditions in frequency range of 57-59 kHz.	34
Figure 2.17: A generic single degree of freedom electro-mechanical	39
Figure 2.18: Idealized 1-D – Structure interaction	40
Figure 2.19: Particle Motion of Elastic Waves	45
Figure 2.20: Piezoelectricity Effect	47
Figure 3.1: Elastically constrained 1-D PZT-structure interaction model.	53
Figure 3.2: Freely suspended PZT patch (10 mm x 10 mm x 0.3 mm thickness)	56

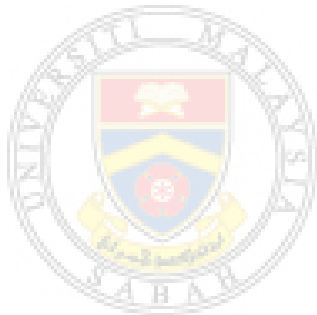
Figure 3.3:	Plot of admittance signatures versus frequency (0-1000 kHz) derived analytically from freely vibrating PZT transducer with varying length, l (a) Conductance (b) Susceptance	57
Figure 3.4:	Plot of admittance signatures versus frequency (0-1000 kHz) derived analytically from freely vibrating PZT transducer with varying thickness, h (a) Conductance (b) Susceptance	58
Figure 3.5:	Plot of admittance signatures versus frequency (0-1000 kHz) derived analytically from freely vibrating PZT transducer with varying density, ρ (a) Conductance (b) Susceptance	59
Figure 3.6:	Plot of admittance signatures versus frequency (0-1000 kHz) derived analytically from freely vibrating PZT transducer with varying Young's modulus, Y_{11}^E (a) Conductance (b) Susceptance	60
Figure 3.7:	Plot of admittance signatures versus frequency (0-1000 kHz) derived analytically from freely vibrating PZT transducer with varying Poisson ratio, ν (a) Conductance (b) Susceptance	61
Figure 3.8:	Plot of admittance signatures versus frequency (0-1000 kHz) derived analytically from freely vibrating PZT transducer with varying mechanical loss factor, η (a) Conductance (b) Susceptance	62
Figure 3.9:	Plot of admittance signatures versus frequency (0-1000 kHz) derived analytically from freely vibrating PZT transducer with varying electric permittivity, E_{33}^T (a) Conductance (b) Susceptance	63
Figure 3.10:	Plot of admittance signatures versus frequency (0-1000 kHz) derived analytically from freely vibrating PZT transducer with varying electrical loss factor, δ (a) Conductance (b) Susceptance	64

Figure 3.11:	Plot of admittance signatures versus frequency (0-1000 kHz) derived analytically from freely vibrating PZT transducer with varying piezoelectric strain coefficient, d_{31} . (a) Conductance (b) Susceptance	65
Figure 3.12:	Conductance signatures versus frequency from freely vibrating PZT transducer (comparison between experimental and analytical).	66
Figure 4.1:	Pictorial illustration of experimental setup for EMI technique.	71
Figure 4.2:	PZT patch surface bonded on specimen	72
Figure 4.3:	Section view of PZT patch configurations on Mortar Specimen	72
Figure 4.4:	Prism PE1 with two embedded PZT patches at 75 mm distance from prism centre line	74
Figure 4.5:	Section view of PZT patches, BE1 & BE2 Configurations on Mortar Specimen, PE1	74
Figure 4.6:	Section view of PZT patch, BE3 Configurations on Mortar Specimen, PE2	75
Figure 4.7:	Conductance signatures versus frequency acquired from patch PR (room condition) in the frequency range of 0 – 900 kHz.	76
Figure 4.8:	Conductance signatures versus frequency acquired from patch PR (room condition) in the frequency range of 100 – 300 kHz	77
Figure 4.9:	Frequency of first PZT's resonance against time for all samples.	78
Figure 4.10:	Conductance signatures versus frequency acquired from patch PR (room condition).	79
Figure 4.11:	Frequency of resonance peak (26.5 kHz at day 1) against time for samples PR and PS.	80

Figure 4.12:	Conductance signatures versus frequency acquired from embedded patch BE1 in the frequency range of 70 – 110 kHz.	81
Figure 4.13:	Conductance signatures versus frequency acquired from embedded patch BE2 in the frequency range of 70 – 110 kHz.	82
Figure 4.14:	Conductance signatures versus frequency acquired from embedded PZT patch for Prism PE2 submerged in water (frequency range of 10 – 400 kHz).	83
Figure 5.1:	Diagram of Surface Wave Propagation Approach	86
Figure 5.2:	Example of 10 kHz, 5-count tone burst excitation: (a) raw tone burst, (b) Smoothed tone burst	87
Figure 5.3:	Configurations of PZT patches for (a) Prism A (Rough Surface) (b) Prism B (Smooth Surface)	89
Figure 5.4:	Section view of PZT patches Configurations on Mortar Specimen.	89
Figure 5.5:	Experimental Setup for Surface wave propagation on Mortar Specimen	90
Figure 5.6:	Estimate time of arrival using cross correlation	92
Figure 5.7:	Using Hilbert Transform to construct the envelope of a 3-count, Hanning windowed sinusoidal signal	93
Figure 5.8:	Envelope of a signal represents the amplitude of the signal	93
Figure 5.9:	Distribution of cross correlation and Hilbert Transform's envelope against time for Prism A at 30 kHz and 100 mm Actuator-Sensor distance.	94
Figure 5.10:	Surface wave packet and TOF (Sensor's amplitude is scaled by a factor of 100 for better schematic comparison with the actuator signal)	95

Figure 5.11:	Amplitude of actuator and sensor versus time step for Prism A at 30 kHz after 1 day	97
	(a) Actuator-Sensor Distance: 60 mm (Prism A)	
	(b) Actuator-Sensor Distance: 100 mm (Prism A)	
	(c) Actuator-Sensor Distance: 160 mm (Prism A)	
Figure 5.12:	Amplitude of actuator and sensor versus time step for Prism B at 30 kHz after 1 day	99
	(a) Actuator-Sensor Distance: 60 mm (Prism B)	
	(b) Actuator-Sensor Distance: 100 mm (Prism B)	
	(c) Actuator-Sensor Distance: 160 mm (Prism B)	
Figure 5.13:	Wave Speed versus Curing Time for Prism A and Prism B at Frequency of 30 kHz.	101
	(a) Prism A and Prism B, 30 kHz, Actuator-Sensor Distance: 60mm	
	(b) Prism A and Prism B, 30 kHz, Actuator-Sensor Distance: 100mm	
	(c) Prism A and Prism B, 30 kHz, Actuator-Sensor Distance: 160 mm	
Figure 6.1:	Experimental Setup for Surface wave propagation on Concrete Specimen	104
Figure 6.2:	Wires Soldered on PZT Patch	105
Figure 6.3:	Concrete Mixed inside Concrete Mixer	106
Figure 6.4:	Configurations of PZT patches on Concrete Specimen	107
Figure 6.5:	Section view of PZT patches Configurations on Concrete Specimen.	107
Figure 6.6:	Concrete Cubes and Concrete Prism	108
Figure 6.7:	Curing of Concrete Cubes Submerged in Water	109
Figure 6.8:	Weighing of Concrete Cube	109
Figure 6.9:	Concrete Cube Compressive Test	110

Figure 6.10:	Amplitude of actuator and sensor versus time step for Concrete Prism at 30 kHz after 1 day	111
	(a) Actuator-Sensor Distance: 60 mm (Concrete Prism)	
	(b) Actuator-Sensor Distance: 100 mm (Concrete Prism)	
	(c) Actuator-Sensor Distance: 160 mm (Concrete Prism)	
Figure 6.11:	Wave Speed versus Curing Time for Concrete Specimen with Actuator-Sensor Distance of 60 mm, 100 mm and 160 mm at Frequency 30 kHz.	113
Figure 6.12:	Average Wave Speed versus Curing Time for Concrete Specimen.	114
Figure 6.13:	Correlation of Dynamic Modulus of Elasticity and Compressive Strength of Concrete Cubes.	116



UMS
UNIVERSITI MALAYSIA SABAH

LIST OF ABBREVIATION

ASTM	-	American Society for Testing and Materials
BS	-	British Standard
BS EN	-	British Standard European Norm
EMI	-	Electromechanical Impedance
IEEE	-	The Institute of Electrical and Electronics Engineers
MS	-	Malaysian Standard
NDE	-	Non-Destructive Evaluation
PVDF	-	Polyvinylidene Fluoride
PWAS	-	Piezoelectric Wafer Active Sensors
PZT	-	Lead Zirconate Titanate
RMSD	-	Root Mean Square Deviation
SASW	-	Spectral Analysis of Surface Waves
SEF	-	Static Equivalent - Force
SHM	-	Structural Health Monitoring
SMA	-	Shape Memory Alloys
TOF	-	Time of Flight
UPV	-	Ultrasonic Pulse Velocity

LIST OF SYMBOLS

A_a	-	Cross sectional area of PZT patch
A	-	Constant mass matrix multiplier
b_a	-	Width of actuator
C	-	Electrical capacitance of PZT patch
d	-	Distance
d_{31}	-	Piezoelectric constant of PZT patch
d_c	-	Strain coefficient tensors (converse)
d_d	-	Strain coefficient tensors (direct)
$[d^c]$	-	Piezoelectric strain coefficient tensors (converse)
$[d^d]$	-	Piezoelectric strain coefficient tensors (direct)
δ	-	Electrical loss factor
D_3	-	Electric charge density on surface normal to axis 3 of PZT
D_i	-	Electric displacement
$[D]$	-	Electric displacement vector
E	-	Young's modulus of elasticity
E_3	-	Electric field applied along axis 3 of PZT patch
E_j	-	Applied external electric field
$[E]$	-	Applied external electric field vector
$\overline{\epsilon_{33}^T}$	-	Complex dielectric constant at zero stress
$[\overline{\epsilon^T}]$	-	Complex dielectric permittivity tensor
f	-	Frequency
g_{31}	-	Piezoelectric voltage constant
γ	-	Wave number
$H(x(t))$	-	Hilbert Transform
h	-	Thickness of PZT patch
h_a	-	Thickness of Actuator
i	-	Reference signature at different frequencies
j	-	Imaginary number
j	-	Amount of lag (in cross correlation)

k_{31}	- Coupling factor
K_{etr}	- Dynamic Stiffness of Host Structure
K_{PZT}	- Quasi-static stiffness of PZT patch
k	- Wave number
l	- Length of PZT patch
l_a	- Length of Actuator
λ	- Wavelength
ω	- Angular frequency
Φ	- Admittance poles
ϕ	- Displacement phase shift (phase angle)
η	- Mechanical loss factor
$p_{12}(j)$	- Cross Correlation
ρ	- Density
R	- Stiffness ratio
$R_{xy}(t)$	- Cross Correlation of two signals $x(t)$ and $y(t)$
s_{11}^E	- Elastic constant along axis 1 at zero electric field
$[S^E]$	- Complex elastic compliance tensor
S_1	- Strain of the PZT patch in direction 1
$[S]$	- Strain tensor
t	- Time
θ	- Angular Coordinate
τ	- Time step (Hilbert Transform)
T	- Curie temperature
T_1	- Stress applied in the direction 1
$[T]$	- Stress tensor
V	- Wave Velocity
V_p	- P-wave Velocity
V_s	- S-wave velocity
V_R	- Rayleigh wave velocity
$V(t)$	- Sinusoidal voltage applied
\bar{V}	- Voltage applied (in complex notation)

ν	- Poisson ratio
ν_a	- Poisson ratio of actuator
w	- Width of PZT patch
$X_1(n)$	- Data sequence 1
$X_2(n)$	- Date sequence 2
$x(t)$	- Input signal
\bar{Y}	- Complex electrical admittance
\bar{Y}_{11}^E	- Complex Young's modulus of PZT patch along axis 1 at zero electric field
Z	- Mechanical impedance of host structure
$Z_{i,1}$	- Baseline admittance signatures at frequency interval i
$Z_{i,2}$	- Admittance signatures at frequency interval, i with different temperature
Z_a	- Mechanical impedance of actuator
$Z_{a,eff}$	- Effective mechanical impedance of actuator
$Z_{s,eff}$	- Effective mechanical impedance of host structure
Z_{axx}	- Mechanical impedance of actuator in x -direction
Z_{ayy}	- Mechanical impedance of actuator in y -direction
Z_{xx}	- 2-D Mechanical impedance of host structure in x -direction
Z_{yy}	- 2-D Mechanical impedance of host structure in y -direction
Z_{xy}	- 2-D Cross mechanical impedance of host structure in y -direction
Z_{yx}	- 2-D Cross mechanical impedance of host structure in x -direction

LIST OF APPENDICES

	Page
Appendix A: Matlab Code to Calculate the Analytical Value of Electrical Admittance of PZT	133
Appendix B: Matlab Code to Compute the Cross Correlation and Hilbert Transform Methods.	135
Appendix C: Some of the Experimental Results from the Surface Wave Propagation Method. (Actuator/Sensor vs Time Readings for Prism A, 30 kHz, Actuator – Sensor Spacing: 160 mm)	138



UMS
UNIVERSITI MALAYSIA SABAH